Indian Journal of Fibre & Textile Research
Vol. 51, March 2026, pp. 67-73
DOI: 10.56042/ijftr.v51i1.18902

Up-scaling of polyvinylidene fluoride electrospun nanofibres with a needleless wire spinneret technique

Komal Kukreja[1,2], Prasanna Kumar S Mural[1,a] & Prasanta K Panda[2,b]

[1]Department of Metallurgical Engineering & Materials Science, Indian Institute of Technology, Mumbai 400076, India
[2]Bombay Textile Research Association, Ghatkopar West, Mumbai 400086, India

Received 18 April 2025; revised received and accepted 10 November 2025

Polyvinylidene fluoride (PVDF) is a thermoplastic polymer best known for its extraordinary chemical stability, excellent heat and wear resistant, better mechanical properties, easy processability, resistance to hydrolysis and ultraviolet radiation. Due to its electroactive β-phase content responsible for generating voltage in the presence of an external electric field, PVDF has wide application in energy harvesting, energy storage, sensors and actuators. PVDF can be nanospun into fibres through electrospinning process which further helps in the orientation of dipoles and enhancing its property. In this work, PVDF nanofibres were prepared by using needleless wire spinneret technique. Different types of solution parameters such as solution concentration and electrospinning parameters such as voltage, distance between two electrodes was studied. The optimized concentration obtained from the study is 24%, distance between two electrodes is 130 mm and voltage of positive and negative electrode is +40 kV and -15 kV. XRD analysis is done to determine its phase content and DMA analysis was done to study the mechanical behaviour of the prepared fibres.

Keywords: Electrospinning, Nanofibre, Polyvinylidene fluoride

1 Introduction

Polyvinylidene fluoride is thermoplastic piezoelectric- polymer having interesting properties of piezo- and pyro electricity, good mechanical properties and chemical resistance. Today PVDF has become the second largest volume fluoro polymer after polytetrafluoroethylene. It exhibit excellent piezoelectric properties having great opportunities to be used in polymer composites and composite fibres[1]. It can convert mechanical energy of body motion and the surrounding environment to electrical energy and vice versa. PVDF exists in four different phases based on the conformations of $–CH_2–$ and $–CF_2–$ in the polymer chain. The main phases are α-, β-, γ- and δ-phase, and a fifth hypothetical ε-phase. Polar β-phase consists of all trans-conformation which shows piezoelectric response. It is believed that fluorine atoms are statistically offset due to its large size that does not allow simple all trans-conformation[2]. In the presence of an electric field, reorientation of dipoles takes place which generates useful piezoelectric properties. Apart from energy storage and harvesting, PVDF is well-suited for various other applications, such as, gas and liquid separations through membranes, drug delivery, and tissue engineering[3].

With the advancement in nanotechnology, polymers can also be made into nanofibres to improve their properties further. Nanofibres are fibres having diameter in nanoscale lengths. These fibres have a high aspect ratio of more than 1000:1. Compared to the bulk material these fibres have a high specific surface area, good flexibility, high surface reactivity and anisotropic physical properties such as mechanical, thermal, electrical and conductivity. Other important characteristics of the nanofibres include optical transparency, low cost, and good mechanical flexibility/strength, and conductive nanofibres have good electrical conductivity. These features make these materials to be applied in the next generation of energy conversion and storage devices with high energy/power density, transparency, portability, and flexibility[1].

Electrospinning is a cost effective and adaptable technique for producing nanofibres. In a conventional electrospinning process, polymer solution is taken in a needle and high positive voltage is applied across the polymer solution and a ground voltage is applied across the substrate or nanofibrecollector by which an

[a]Corresponding author.
E-mail: prasannamural@iitb.ac.in, nanolab@btraindia.com

electric field is generated. When the surface tension of the air-polymer interface is overcome by the electric field force of the accumulated ions on the polymer, the polymer jet begins. At the needle tip, a conical shape droplet region called Taylor cone is formed due to balance between surface tension and electrostatic force. Then a stable region is there followed by an unstable whipping motion region forming a jet with a cone shape opening near the collector[4-6]. However the production capacity of this process is low, i.e, less than 0.3 g/h[7]. By increasing the number of needles, the production capacity can be increased, but blockage in needles leads to discontinuity in fibres[8].With time various types of unconventional spinning method such as disk[9], drum[10], rotary cone[11] have been developed. The working principle of each process is different and requires process optimization. The latest advancements in needleless electrospinning have effectively overcome the limitations of low throughput from needle-based electrospinning. Needleless electrospinning can generate abundant polymer droplets without requiring a needle, in which an electric field is applied between the droplets and the conductive collector. Fibreproperties depends on solution properties such as molecular weight, concentration, viscosity, conductivity and surface tension as well as electrospinning process parameters such as flow rate, supply voltage, and distance between electrodes, and ambient parameters consist of temperature, airflow, and moisture.

Electrospun PVDF nanofibres has application in clean energy and sustainability, energy harvesting, water treatment, gas separation and environmental sensing that helps to create a sustainable future towards clean energy, water, and air. PVDF nanofibres and its copolymers have been widely used to fabricate ultrafiltration (UF) and microfiltration (MF) membranes. Its typical copolymers include poly(vinylidene fluoride-cochlorotrifluoroethylene) (PVDF-CTFE), poly(vinylidene fluoride-co-tri-fluoro-ethylene) (PVDF-TrFE), and poly-(vinylidene-fluorideco-hexafluoropropylene) (PVDF-HFP), and they are known for their unique ferroelectric, pyroelectric and piezoelectric properties associated with different phases and structures. The PVDF homopolymer consists of 59.4 wt% fluorine and 3 wt% hydrogen. The van der Waals radius of fluorine atoms (1.35 Å) differs from that of hydrogen (1.2 Å). Due to the difference in electro negativity between carbon and fluorine atoms within the polymer chain [$–CH_2–CF_2–$], compared to that between carbon and hydrogen atoms creates a dipole moment perpendicular to the monomer chain[12], which is important for its piezoelectric property. Electrical polling and mechanical stretching during electrospinning lead to the elongation of the twisted PVDF chains and promote alignment along the Fibreaxis, which enhances the formation of the β phase and creation of piezoelectric properties.

Electrospunnano fibres possess high specific surface area, large aspect ratios, flexibility, stretchability, and enhanced pore interconnectivity, making them highly suitable for energy harvesting applications. Mechanical motions such as bending, twisting, multi-directional stretching, and pressing can be converted into electrical energy to power low-consumption wearable sensors[13]. PVDF electrospunfibres and their copolymers are promising as separators in Li-ion batteries due to their high porosity and specific surface area, which improve electrolyte uptake and, consequently, the electrochemical performance of the battery[14]. Additionally, PVDF electrospun membranes are effective for water treatment and air filtration owing to their interconnected pore structure[15,16]. They are also widely explored for environmental sensing applications, including gas detection, water quality monitoring, temperature sensing, humidity measurement, and light sensing[17].

In this work, a wire spinneret was used as an electrode in needleless electrospinningto produce PVDF nanofibres. The effect of polymer concentration, applied voltage, and thespinning distance on electro-spunfibres was studied. SEM analysis was done to examine the fibres quality. XRD and DMA analysis were done for the optimized PVDF fibres to study the crystalline phases and mechanical property of the nanofibres.

2 Materials and Methods

2.1 Materials

PVDF granules of grade Kynar 710 (Melt Viscosity 4-8 poise @ 230°C and 100 sec^{-1}, melt flow rate 19-35 g/10 min @ 230°C, Melting point 165-172 °C) was purchased from Arkema Chemicals, Mumbai. The analytical grade Dimethyl formamideas a solvent were procured from Merck Limited, Mumbai. Polypropylene spun-bonded nonwoven fabric as a deposition substrate was purchased from Techfab (India) Industries Ltd., Daman, India.

2.2 Methods

2.2.1 Solution Preparation

The required amount of PVDF granules were mixed with solvent Dimethyl formamide (DMF) to prepare 15, 20, 24 and 27 weight percentage of solution. The solution was prepared by mixing with magnetic stirring at temperature 60°C for 2 h.

2.2.2 Electrospinning Process

PVDF nanofibres from different weight percentage of spinning solution were prepared with needleless wire electrospinning technique (NS 1W500U, Elmarco, Czech Republic). During electrospinning, temperature was maintained at 28±1°C and relative humidity at 40±1%. Distance between positive and negative electrode were also varied as 130, 150, 170 and 190 mm.Voltage between positive and negative electrodes were also varied as 40/15, 40/20, 40/25, 45/15, 50/15 (+kV/-kV). Other spinning parameters containing carriage speed (150 mm/s), positive electrode speed (2 mm/min), orifice diameter (0.7 mm), inlet air (60 m^3/h), outlet air (90m^3/h) and deposition time of 2 min were kept constant during electrospinning. The needleless electrospinning setup is shown in Fig. 1. In it, polymer is taken by the carrier on a wire electrode. The positive voltage is applied across the wire electrode with polymer and negative voltage is applied across the collector side. When the surface tension on the polymer at the air polymer interface is overcome by the electrostatic field force, polymer jet began to flow in the form of nanofibres and get deposited on spun bonded polypropylene nonwoven fabric.

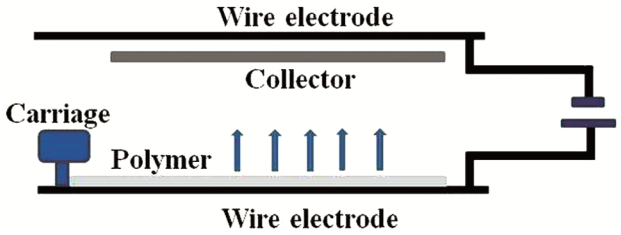

Fig. 1 — Needleless electrospinning process

2.3 Characterization

Surface morphologies of the prepared samples were observed under the scanning electronmicroscope (JEOL JSM IT200 LV, Japan) after goldsputter coating (JEOL JEC-550 Twin coater). The diameter of the samples was measured from imagej software. The mean diameter and standard deviation of 150 readings were calculated. To determine the structural details of optimized samples, X-ray diffraction study was done using X'Pert PRO PANalytical instrument. To determine the effect of deformation on its various properties such as piezoelectric response, durability and resistance to deformation, Dynamic mechanical measurements of the optimized sample were done using Discovery DMA850 instrument.Initially tensile test was done to determine the maximum load taken by the nanofibres. Then amplitude sweep was performed from 0.00001 mm to 10 mm with an increment of 10 micron at 1 Hz frequency with 0.5 N pre-load to determine the linear viscoelastic region of the sample. Temperature sweep was performed from room temperature to 165°C with a ramp rate of 5°C/min at a frequency of 10 Hz, amplitude of 0.01 mm and pre-load of 0.05 N. This helps in understanding the flexibility of fibre, comfort and its behaviour under stress.

3 Results and Discussion

The SEM image of the prepared nanofibres at different conc. of 15, 20 and 24 wt% with 10000 magnifications is shown in Fig. 2. The distance between two electrodes was 130 mm and applied voltage on two electrodes was +40 kV and -15 kV. At 27 wt%, the viscosity of the solution is high to spin the fibres. At 15 wt% concentration, polymer droplets

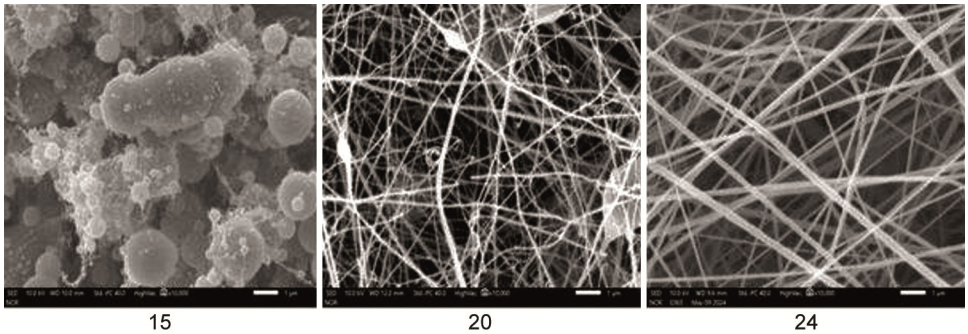

Fig. 2 —SEMimage of nanofibres prepared with different polymer concentration (wt%)

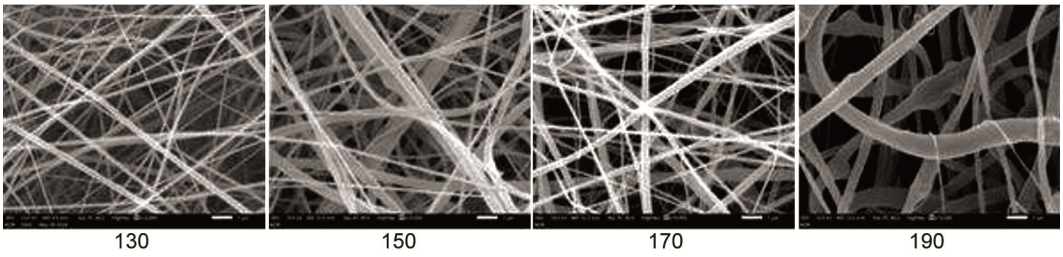

Fig. 3 —SEMimages of nanofibres prepared with different distance (mm) between the electrodes

are formed during spinning which is the characteristic of electrospraying process. It shows that this concentration does not have sufficient polymer molecular chain entanglements for spinnability. This concentration is not ideal for the formation of homogeneous fibres and the boundary concentration between electrospraying and electrospinning is between 15 to 20 %[18]. At 20 wt%, fibres are formed with beaded structure, which shows that chain entanglements are sufficient enough for the formation of fibres[19]. At 24 wt%, more uniform and smooth fibres are formed. This is because with increase in concentration, the interaction between polymer chains and solvent molecules increased in the presence of external field and distributed over the entangled polymer molecules decreasing aggregation of solvent molecules thus preventing bead formation of the fibres[20]. However further increasing the concentration to 27% leads to high viscous solution with which spinning could not take place. The average diameter of fibres formed with 24 wt% is 125.7 nm with standard deviation of 43.2. Hence 24 wt% is considered for further study.

At 24 wt.% concentration, distance between two electrodes was increased from 130 to 150, 170 and 190 mm. Applied voltage on two electrodes was +40 kV and -15 kV. The SEM images of the prepared samples are shown in Fig. 3. The average diameter and standard deviation is shown in Table 1 and diameter histogram is shown in Fig. 4. The diameter and standard deviation of the prepared samples increased with increased in distance between them as overall charge density between the electrodes reduces cause less electrostatic force experienced by the fibres. This leads to slower Fibre stretching and thicker fibres. However very short distance lead to instability in the process. In this process of electro spinning, 130 mm is the minimum and optimized distance at +40 kV and -15 kV voltage. Thus 130 mm is considered for further study.

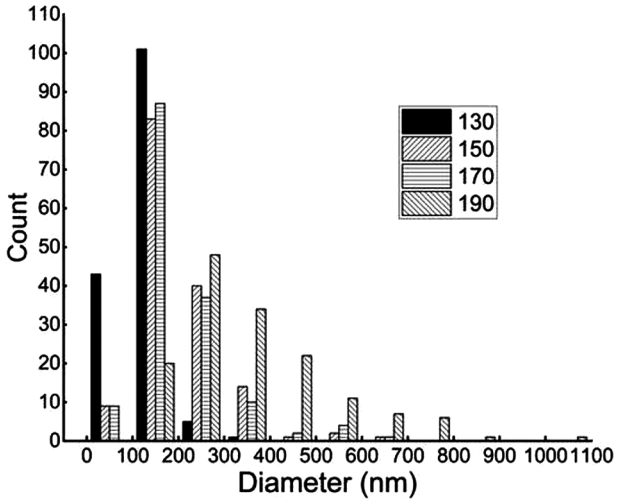

Fig. 4 — Histogram of diameter of nanofibres prepared with different distance between electrodes

Table 1 —Average diameter and standard deviation of diameter of nanofibres prepared with different distance between electrodes

Distance, mm	Average Diameter, nm	Standard Deviation
130	125.7	43.2
150	194.0	90.7
170	196.8	104.38
190	357.4	171.0

Table 2 — Average diameter and standard deviation of diameter of nanofibres prepared with different voltage between electrodes

Voltage, +kV/-kV	Average Diameter, nm	Standard deviation
40/15	125.7	43.2
40/20	141.8	54.4
40/25	212.4	131.0
45/15	128.8	44.6
50/15	159.9	82.4

The SEM images of the fibres prepared with different voltage are shown in Fig. 5. The average diameter and standard deviation is shown in Table 2 and diameter histogram is shown in Fig. 6. With increase in positive voltage from +40 kV to +45 kV, keeping negative voltage of -15 kV, the average Fibre diameter increased only marginally (125.7 ± 43.2 nm

Table 3 — Anova analysis for the diameter of nanofibres prepared +40/-15 and +45/-15 voltage

Source of Variation	Sum of squares	Degree of freedom	Mean Square	F-statistic	P-value	Critical F-value
Between Groups	706.689	1	706.689	0.367	0.545	3.873
Within Groups	573440.447	298	1924.297			
Total	574147.136	299				

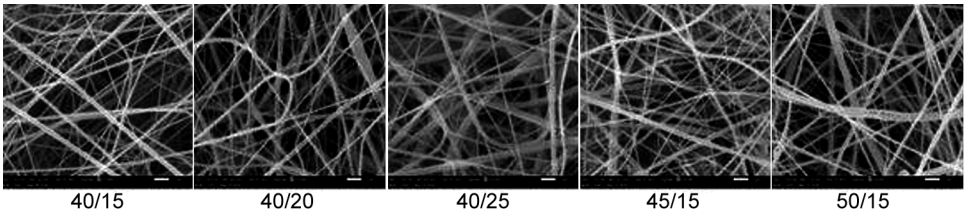

Fig. 5 — SEMimages of nanofibres prepared with different voltages between the electrodes (+kV/-kV)

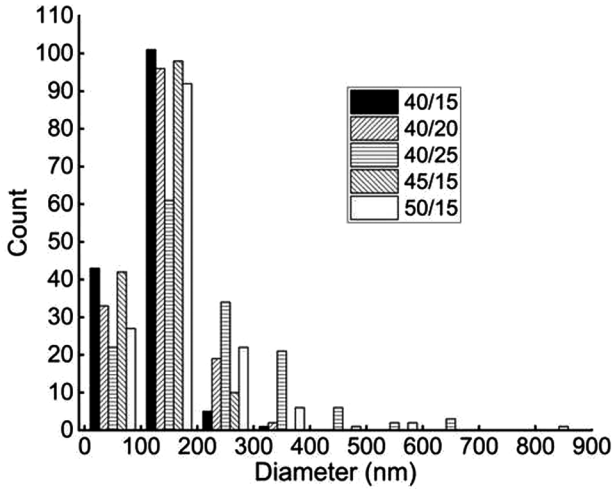

Fig.6 — Histogram of diameter of nanofibres prepared with different voltage between electrodes

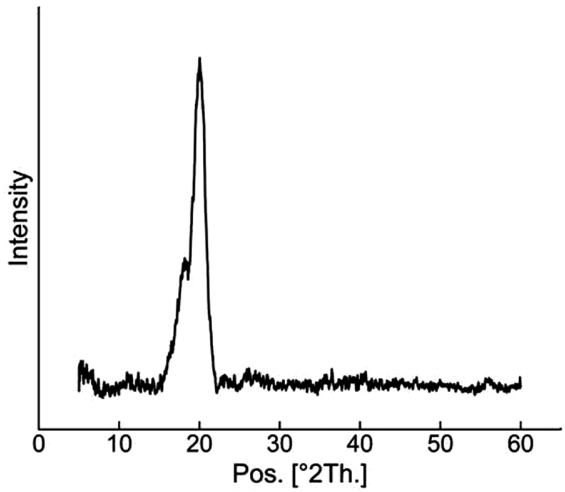

Fig.7 — XRD pattern of optimized nanofibres

vs. 128.8 ± 44.6 nm) which are very close. To address this, statistical ANOVA analysis was performed whose summary is shown in Table 3. The p value obtained is 0.54 which is greater than 0.05 and itconfirmed that the difference between the two conditions is not statistically significant**.** The diameter distributions from figure 6 are consistent with these results, showing comparable dispersion for both voltages. A further increase in positive voltage upto +50 kV leads to small increase in Fibrediameter. Similarly with increase in negative voltage from -15 to -20 and -25 kV, Fibrediameter and standard deviation increases. This is because increase in voltage difference beyond a limit leads to instability in jet and forms more non uniform fibres. Voltage of +40/−15 kV is selected as the optimum condition because it achieves the same Fibremorphology at a lower applied voltage, making the process more energy-efficient and stable in long-term electro-spinning.

The XRD analysis of the optimized fibres prepared with 24wt.% concentration, distance between electrodes 130 mm and voltage applied across electrodes +40 kV/-15 kV is shown in Fig. 7. Peak at 18.17° corresponds to the diffraction of alpha phase for the crystal plane of (020) and (100), while peak at 20.05° corresponds to the diffraction of beta phase for the crystal plane of (110) and (200)[21]. The overall crystallinity of the sample is 35.49%. The peaks were deconvoluted between 15° to 22° is shown in Fig. 8. The area of the peaks was used to calculate the crystallinity of corresponding phases using the formula as shown in equation 1 and equation 2[21].

$$\chi\alpha(\%) = \frac{A\alpha}{A\alpha+A\beta} X\, \chi \quad \ldots(1)$$

$$\chi\beta(\%) = \frac{A\beta}{A\alpha+A\beta} X\, \chi \quad \ldots(2)$$

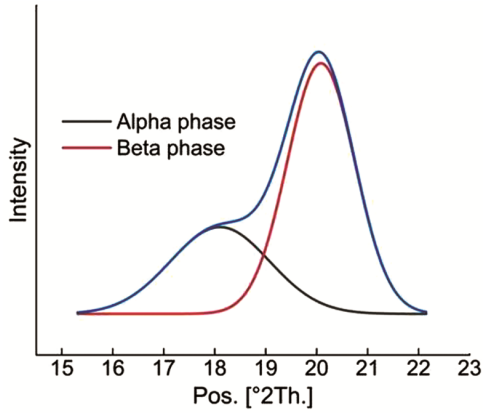

Fig. 8 — Deconvoluted graph of XRD of nanofibres

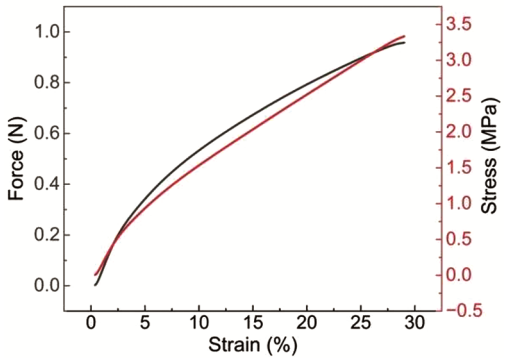

Fig. 9 — Stress strain graph of PVDF nanofibre

where A is the area of the peak and χ is the crystalinity. The crystallinity of alpha phase is 11.95 % while that of beta phase is 23.54%. The beta phase dominates over alpha phase due to the orientation of dipoles of $–CH_2-CF_2-$ group and stretching experienced by the polymer chains in the presence of external field.

The stress strain graph for the prepared nanofibres is shown in Fig. 9. The max force material can withstand is 0.95 N and stress of 3.3 Mpa. Amplitude sweep graph is shown in Fig. 10. The storage modulus of the sample is higher than the loss modulus shows the gel like structure for viscoelastic behaviour. Upto 0.01 mm, there is a linear viscoelastic region, after which there is gradual decrease in storage modulus due to the breakdown of structure. Temperature sweep data of storage and loss modulus is shown in Fig. 11. Its tan delta graph is shown in Fig. 12. A large deformation is observed between 40^{O}C to 160^{O}C that corresponds to the alpha phase relaxation behaviour[22]. This is associated with motions within the crystalline fraction. This relaxation is not clearly observed as a peak in the tan δ plot. This may be a

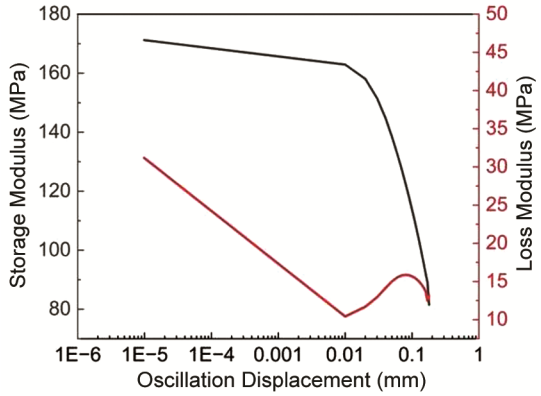

Fig. 10 —Amplitude sweep graph of PVDF nanofibre

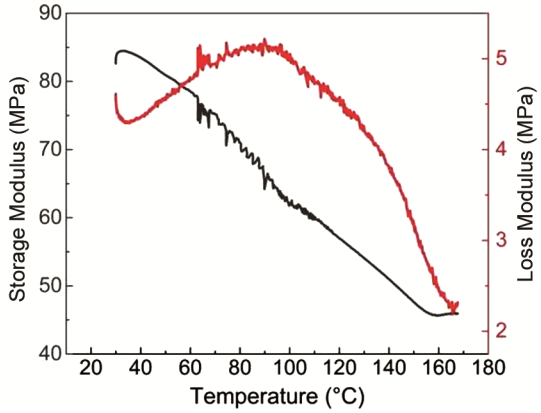

Fig. 11 — Temperature sweep graph of PVDF nanofibre

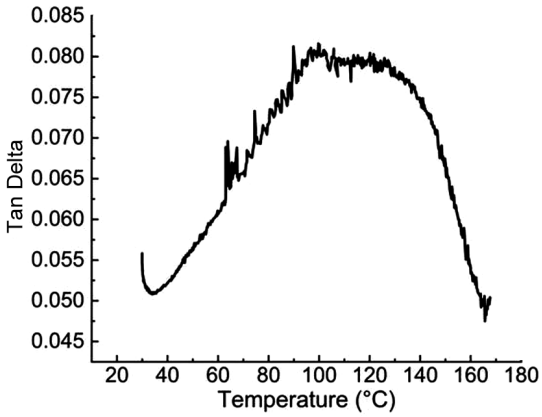

Fig. 12 — Tan delta graph of PVDF nanofibre

result of the morphology of highly oriented crystalline fraction in the fibres. This process is similar to the alpha phase relaxation of polyethylene in which diffusion of polymer chains in the amorphous region takes place. A rotational and translation motion within the chain takes place involving 180°flip motions of the chain stems in the crystalline lamellae[23].

4 Conclusion

PVDF polymer was successfully spun using the needleless electrospinning process. The influence of polymer concentration, applied voltage, and spinning distance on Fibremorphology and diameter was systematically investigated. Optimal conditions—24 wt.% polymer concentration, 40 kV/–15 kV applied voltage, and 130 mm spinning distance-produced uniform fibres with minimal bead formation. XRD analysis revealed a total crystallinity (χ) of approximately 35.5%, of which the α-phase comprised ~12.0% (χ_α ~11.95 %) and the β-phase ~23.5% (χ_β ~23.54 %). It confirmed the predominance of the β-phase, with its content approximately twice that of the α-phase. The β-phase, being more electroactive and piezoelectric, is preferentially formed under electrospinning conditions, where stretching and electric field exposure favor transformation from the nonpolar α-phase. The sample exhibited a clear linear viscoelastic region up until approximately 0.01 mm displacement, where the storage modulus (G′) remained stable—indicating robust elastic response. Beyond that, G′ gradually declined, signifying structural yielding and transition to non-linear viscoelastic behavior. This result is characteristic of polymeric materials and is effectively captured using DMA, which differentiates elastic (storage modulus) from viscous (loss modulus) contributions. Our results support the understanding that needleless electrospinning is a highly effective method for maximizing PVDF's electroactive crystalline content.

Acknowledgements

The authors wish to acknowledge the valuable assistance provided by Metallurgical Engineering and Materials Science Department, Indian Institute of Technology and Bombay Textile Research Association.

References

1 Chinnappan A, Baskar C, Baskar S, Ratheesh G & Ramakrishna S, *J Mater Chem C*, 5 (48) (2017) 12657.
2 Kepler R G & Anderson R A, *Adv Phys*, 41 (1) (1992) 1.
3 Aghayari S, *Heliyon*, 8 (11) (2022) e11620.
4 Matlock-Colangelo L & Baeumner A J, *Lab Chip*, 12 (15) (2012) 2612.
5 Zeng W, Shu L, Li Q, Chen S, Wang F & Tao X. M, *Adv Mater*, 26 (31) (2014) 5310.
6 Zhong J, Zhang Y, Zhong Q, Hu Q, Hu B, Wang Z L & Zhou J, *ACS Nano*, 8 (6) (2014) 6273.
7 Niu H & Lin T, *J Nanomater*, 2012 (2012) 725950.
8 Theron S A, Yarin A L, Zussman E & Kroll E, *Polymer (Guildf)*, 46 (9) (2005) 2889.
9 Ng J J & Supaphol P, *J Polym Res*, 25 (7) (2018) 155.
10 Khan W S, Asmatulu R, Ceylan M & Jabbarnia A, *Fibres Polym*, 14 (8) (2013) 1235.
11 Lu B, Wang Y, Liu Y, Duan H, Zhou J, Zhang Z, Wang Y, Li X, Wang W, Lan W & Xie E, *Small*, 6 (15) (2010) 1612.
12 Wan C & Bowen C R, *J Mater Chem A*, 5 (7) (2017)3091.
13 Mokhtari F, Foroughi J, Zheng T, Cheng Z & Spinks G M, *J Mater Chem A*, 7 (14) (2019) 8245.
14 Bicy K, Gueye A B, Rouxel D, Kalarikkal N & Thomas S, *Surfaces and Interfaces*, 31 (2022) 101977.
15 Kugarajah V, Ojha A K, Ranjan S, Dasgupta N, Ganesapillai M, Dharmalingam S, Elmoll A, Hosseini S A, Muthulakshmi L, Vijayakumar S, Mishra B N, *J Environ Chem Eng*, 9 (2) (2021) 105107.
16 Yang F, Li Y, Yu X, Wu G, Yin X, Yub J & Ding B, *RSC Adv*, 6 (90) (2016) 87820.
17 Kang S, Zhao K, Yu D. G, Zheng X & Huang C, *Adv FibreMater*, 4 (3) (2022) 404.
18 Costa L M M, Bretas R E S & Gregorio R, *Mater Sci Appl*, 01 (4) (2010) 247.
19 Ruan L, Yao X, Chang Y, Zhou L, Qin G & Zhang X, *Polymers (Basel)*, 10 (3) (2018) 1.
20 Ray S S, *Processing of Polymer-based Nanocomposites Processing-structure-property-performance relationships*, 278 (2018).
21 Pratihar S, Chandran A M, Bhat A R & P K S Mural, *ACS Appl Nano Mater*, 7 (17) (2024) 20553.
22 Liu Z, Maréchal P & Jérôme R, *Polymer (Guildf)*, 38 (19) (1997) 4925.
23 Mano J F, Sencadas V, Costa A M & Lanceros-Méndez S, *Mater Sci Eng A*, 370 (2004) 336.